

## $\gamma$ Irradiation effects on optical, thermal, and mechanical properties of polysulfone/MWCNT nanocomposites in argon atmosphere

Soumen Kumar Ghosh,<sup>1,2</sup> Tapan Kumar Chaki,<sup>2</sup> Dipak Khastgir,<sup>2</sup> Richard Pinto<sup>1</sup>

<sup>1</sup>MECS, PMPD, Systems Reliability Group, ISRO Satellite Centre, Bangalore 560017, Karnataka, India

<sup>2</sup>Rubber Technology Centre, Indian Institute of Technology Kharagpur, Kharagpur 721302, West Bengal, India

Correspondence to: T. K. Chaki (E-mail: tapan@rtc.iitkgp.ernet.in) and D. Khastgir (E-mail: khasdi@rtc.iitkgp.ernet.in)

**ABSTRACT:** Polymer-based composites find use in many nuclear and space application for their ease of fabrication, tailor made properties and light weight. Certain polymers like PTFE, unfilled polyesters and polyamides are prone to degradation in presence of high energy radiation while polymers like epoxies, polyimides, and poly-ether ether ketone have good stability to ionizing radiation. Incorporation of fillers like carbon nanotubes (CNTs) is likely to improve the radiation resistance of the polymers. In this work, polysulfone (PSU)-based nanocomposites were fabricated using multiwalled carbon nanotube (MWCNT) by solution mixing process. The morphology of the PSU/ MWCNT nanocomposites films were studied using Field Emission Scanning Electron Microscopy (FESEM). The prepared films were subjected to  $\gamma$  radiation in an argon environment (to avoid the effect of air/oxygen). Different techniques were used to understand the radiation-induced changes. Gel Permeation Chromatography (GPC) traces of neat PSU before and after exposure to radiation shows a decrease in molecular weight. Infrared spectroscopy shows changes in chemical structure. Differential Scanning Calorimetry (DSC) thermograms reveal dose-related changes. For neat PSU, a decrease in  $T_g$  was observed with increase in dose. For PSU/ MWCNT nanocomposites, the increase in MWCNT content and dose (up to 1.5 MGy) increased the  $T_g$ . Thermo Gravimetric Analysis (TGA) showed a marginal decrease in thermal stability for pristine PSU as well as PSU/MWCNT nanocomposites with irradiation. Tensile strength increased with increasing MWCNT content but decreased with dose. Elongation at break decreased with MWCNT content as well as radiation dose. © 2015 Wiley Periodicals, Inc. *J. Appl. Polym. Sci.* **2015**, *132*, 42017.

**KEYWORDS:** composites; mechanical properties; optical properties; thermal properties

Received 28 September 2014; accepted 20 January 2015

DOI: 10.1002/app.42017

### INTRODUCTION

Ionizing radiation [both particle ( $e^-$ ,  $p^+$ ,  $n^0$ ) and electromagnetic (UV and  $\gamma$  rays)] have a substantial role in altering the properties of either CNTs or its nanocomposites. Earlier work has been done in order to understand the effect of ionizing radiation on CNTs and its nanocomposites. Irradiation using high energy electrons on CNT has been used to study enhancements in mechanical properties which have been attributed to cross-linking of CNT shells. It has been observed that particle irradiation creates covalent bonds directly between adjacent CNTs.<sup>1–4</sup> Electromagnetic irradiation can lead to either covalent bonding between polymer chains which bridge adjacent CNTs or the enhancement of interactions with interstitial molecules present between adjacent CNTs.<sup>5–8</sup> In the presence of ionizing radiation, effect of medium can play an important role in altering the property of CNT. It has been shown that  $\gamma$  irradiation of MWCNTs in presence of air improved the graphitic order and decreased the inter wall distance but the behavior was contrary in presence of epoxy chloropropane.<sup>9</sup> In another work,<sup>10</sup>

not only a two-fold increase in oxygen content on exposing MWCNTs to  $\gamma$  radiation in air as well as epoxy chloropropane has been reported but also a remarkable increase in  $>C=O$  functional group for irradiation in air while  $-COOR$  groups for irradiation in epoxy chloropropane has also been observed. An increase in Young's modulus and electrical conductivity of macroscopically oriented ropes of SWCNTs was observed when subjected to UV radiation in the presence of dimethyl formamide.<sup>6</sup> This was attributed to the cross-links generated between the SWCNT. Gamma irradiation has also been found to induce interstitial carboxyl like groups between adjacent CNTs thereby increasing shear interactions.<sup>7</sup> The effect of  $\gamma$  radiation on SWCNT in presence of different media: water, air and aqueous ammonia was studied.<sup>11</sup>  $\gamma$ -radiation caused introduction of functional groups like  $-OH$ ,  $-COOH$  in presence of all the media, while the presence of nitrile groups were observed only in presence of ammonia. Further, the lengths of SWCNT were found to be shortened by 50% on exposure to  $\gamma$  radiation. Wu *et al.*<sup>12</sup> grafted on to MWCNT. In this, poly (vinyl alcohol) and

two of its derivatives (dimethylketals), termed as polyvinylacetone to MWCNT in the presence of silver ions where the Ag<sup>+</sup> was simultaneously reduced under  $\gamma$ -ray irradiation in one step. Xu *et al.*<sup>13</sup> carried out in-situ covalent grafting of polystyrene on MWCNTs in the presence of  $\gamma$  radiation in single step. Ultraviolet (UV) irradiation has been observed to induce covalent cross-linking in polymer/CNT materials.<sup>6</sup> The effect of  $\gamma$  radiation has also been studied to evaluate characteristics of a number of polymer/CNT nanocomposites.<sup>14–18</sup>

PSU-based nanocomposites have been used for different applications.<sup>19–21</sup> For effective usage in nuclear and space applications, it would be necessary to understand the effect of ionizing radiation on the characteristics of a material. Degradation of PSU in the presence of ionizing radiation differs in the presence and absence of air/oxygen.<sup>22,23</sup> In space, the effect of oxygen due to ATOX is limited to 650 km and with increase in orbit, the effects are reduced. Considering the above aspects, PSU/MWCNT films (prepared by solution casting process) were subjected to  $\gamma$ -radiation in argon environment (to avoid influence of air) and evaluated for different properties. GPC trace analysis was done for neat PSU before and after irradiation to understand the degradation mechanism (scission or cross-linking). Infrared spectroscopic analysis was done to determine structural changes. DSC and TGA analysis was carried out to evaluate thermal stability. FESEM was used to know the microstructure and morphology. In addition, the mechanical properties were also evaluated.

## EXPERIMENTAL

### Materials

Commercially manufactured polysulfone (Udel P 1700) in granular as well in the form of sheet (125  $\mu\text{m}$  thick) supplied by Solvay Advanced Polymers, India was used in this study. MWCNTs were procured from Helix Material Solution, USA and used as it is. MWCNTs were manufactured by chemical vapor deposition process having carbon content of  $\sim 95\%$ , average diameter of 40–60 nm and length of 0.5–40  $\mu\text{m}$ . Mixture of tetrahydrofuran (THF) and *N*-methyl-2-pyrrolidone (DMF) was used as solvent for PSU and was procured from Merck Specialties Private, India.

### Preparation of Nanocomposites Films

PSU nanocomposite films were prepared by a solution mixing process. Prior to film preparation, PSU and MWCNTs were dried separately in a hot air oven at 120°C for 24 h. At first MWCNTs were dispersed in a solvent mixture of THF and DMF by sonication for one hour in a probe type sonicator (frequency, 22.5 kHz; power, 100 W). Then required amount of PSU was dissolved in solvent mixture of THF and DMF sepa-

rately and then added to MWCNT dispersed in the solvent. The mixed solution was stirred and sonicated for 2 h. Stirring and sonication were done in 5-min interval. Films were prepared by casting the solution and evaporating the solvent at room temperature for overnight. Then the dried films were further heated for 2 h at 50°C, for 1 h at 120°C, and finally vacuum dried at 60°C for 10 h to remove the entrapped solvent.

Three compositions were prepared with 0.5, 1, and 2 wt % of MWCNT. Table I gives the sample identification for the various compositions.

### Exposure to $\gamma$ -Radiation

Exposure to  $\gamma$  radiation was done for the PSU as well as PSU/MWCNT nanocomposite films in an argon atmosphere using <sup>60</sup>Co source. For exposing the samples in argon atmosphere, a specially designed container made from SS 304 and having flow control valve, was used. After keeping the samples in this container, the container closed and was alternately evacuated and filled using 99.9999% pure argon through the flow control valve. Argon was maintained at a pressure of 2 bar in the container throughout exposure to  $\gamma$  radiation to avoid entry of air. The samples received doses of 0.5, 1.0, 1.5, and 2.0 MGy respectively in argon. The dose rate was 24 rads/s (0.24 Gy/s) inside the chamber.

### FESEM

The surface morphology and distribution of nanofillers in the polymer matrices were studied using field emission scanning electron microscope (model Supra 40, Carl Zeiss SMT AG, Oberkochen, Germany) after tensile fracture of the samples. Before microscopic study, fracture surfaces of the samples were gold coated by means of manually operated sputter coater (model SC7620, Polaron Brand, Quorum Technologies Ltd., East Sussex, UK) unit.

### Mechanical Testing

Tensile strength measurements were made with Universal Testing Machine, International Equipments, India with cross head speed of 50 mm/min. according to ASTM – D – 882.

## RESULTS AND DISCUSSION

### GPC Analysis

GPC analysis of PSU before and after exposure to  $\gamma$  radiation is shown in Figure 1. With increase in dose, a shift towards the lower molecular weight is observed. The molecular weight ( $M_n$ ) for unirradiated PSU is found to be  $4.35 \times 10^4$  g/mol which decreased to  $1.98 \times 10^4$  g/mol after 2 MGy of exposure. This is due to chain scission.<sup>24</sup> Table II gives the molecular weight and poly-dispersity index (PDI) for the PSU exposed to different radiation dose.

### FTIR Studies

The IR spectra of PSU exposed to different doses in Argon are shown in Figure 2(a). An overall increase in intensity in the entire spectral range was observed. This indicates degradation of the PSU. The decrease in intensity of the bands at  $\sim 3100$   $\text{cm}^{-1}$  and  $2950$   $\text{cm}^{-1}$  indicates the destruction of benzene ring and fragmentation of  $\text{CH}_3$  – group from the main chain. The band at  $1450$   $\text{cm}^{-1}$  is due to fragmentation of  $\text{CH}_3$ -group to form

**Table I.** PSU/MWCNT Nanocomposites Compositions

Composition	Identification
PSU + 0 wt % MWCNT	PSU 0
PSU + 0.5 wt % MWCNT	PNC 1
PSU + 1 wt % MWCNT	PNC 2
PSU + 2 wt % MWCNT	PNC 3

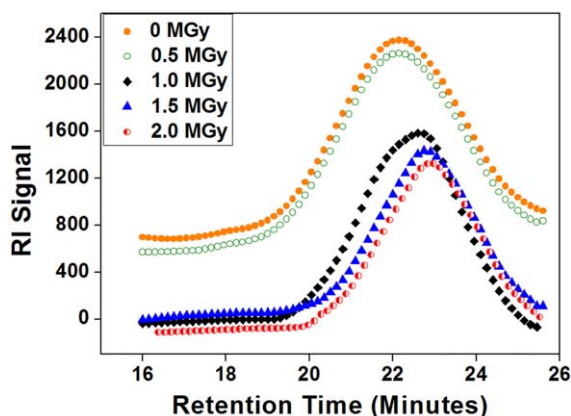


**Figure 1.** GPC analysis of PSU at different dose in Argon. [Color figure can be viewed in the online issue, which is available at [wileyonlinelibrary.com](http://wileyonlinelibrary.com).]

methylene groups. With increase in dose, a new band emerges at  $\sim 1730\text{ cm}^{-1}$ . This is attributed to formation of  $>\text{C}=\text{O}$  group. There are two possible explanations to the creation of carbonyl groups. Degradation causes formation of phenoxy radical [A] and its isomer [B] as shown in Scheme 1. The isomer [B] can abstract hydrogen and form a ketone [C]. Similar observations have been reported by Steckenreiter *et al.*<sup>23</sup> for degradation of polysulfones in presence of ionizing radiation in

**Table II.** GPC Analysis Data

Dose	$M_n$ (g/ mol)	PDI
0 MGy	$4.35 \times 10^4$	1.95
0.5 MGy	$3.13 \times 10^4$	1.93
1.0 MGy	$2.64 \times 10^4$	1.98
1.5 MGy	$2.56 \times 10^4$	2.01
2.0 MGy	$1.98 \times 10^4$	2.06

air as well as vacuum. The other possibility is oxidation of the samples (reactive species) after taking out from argon cannot be ruled out.<sup>25</sup>

The decrease in intensity of the peaks at  $1325$  and  $1290\text{ cm}^{-1}$  is due to fragmentation of sulfone group from the main chain. Also, the decrease in intensity of the peak at  $1230\text{ cm}^{-1}$  is due to degradation of aryl ether group.

In case of PSU/MWCNT nanocomposites, [Figure 2(b–d)], with the increase in radiation dose, none of the compositions showed change in the intensity of the bands at  $\sim 3100\text{ cm}^{-1}$ . This may be due to  $\pi-\pi$  interaction between the aromatic rings of PSU and CNT,<sup>26</sup> which prevents degradation of the aromatic rings. Further, the band occurring at  $1730\text{ cm}^{-1}$  due to  $>\text{C}=\text{O}$  group showed a shift towards  $1680\text{ cm}^{-1}$  with the increase in

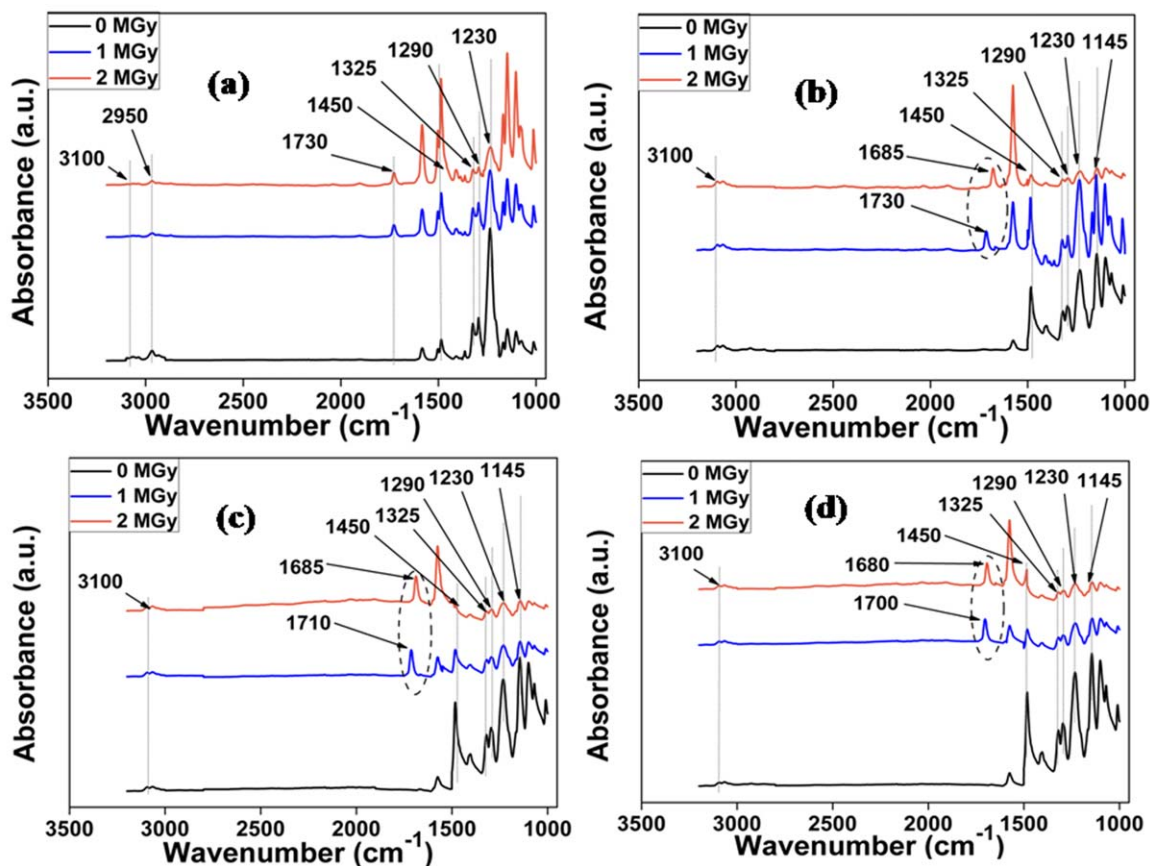
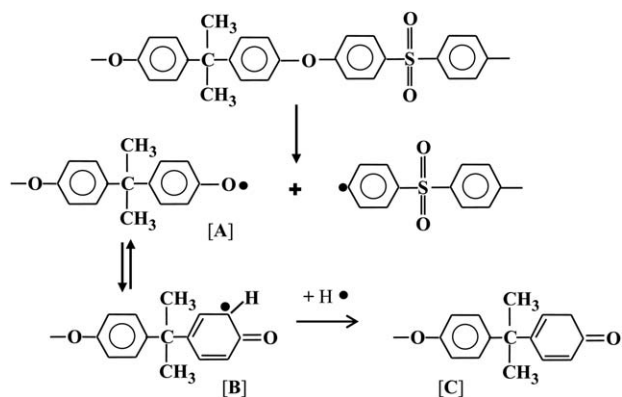


**Figure 2.** Infrared spectra of (a): PSU 0, (b): PNC 1, (c): PNC 2 and (d): PNC 3 at different dose. [Color figure can be viewed in the online issue, which is available at [wileyonlinelibrary.com](http://wileyonlinelibrary.com).]



**Scheme 1.** Degradation mechanism of PSU in presence of  $\gamma$ -radiation.

radiation dose. This is possibly due to the interaction of the  $>C=O$  group with the MWCNT. Fragmentation of  $CH_3$ -group from the PSU due to  $\gamma$ -radiation and generation of different radicals (including formation of methylene group) has been reported by Brown *et al.*<sup>27</sup> and Steckenreiter *et al.*<sup>23</sup> The extent of degradation depends on the dose and may continue till all the  $CH_3$ -groups are eliminated from the PSU chain. It has also been reported that MWCNT act as free radical scavenger.<sup>28–30</sup> The free radicals formed in the PSU main chain during the irradiation process interacts with MWCNT to form linkages. With

increased radiation dose, weakening of the linkage between the free radicals and MWCNT occurs along with fragmentation of more methyl and methylene groups from the PSU chain and hence a decrease in intensity of the peak at  $1450\text{ cm}^{-1}$  is observed. The peaks at  $1325$ ,  $1290$ , and  $1145\text{ cm}^{-1}$  as well as  $1230\text{ cm}^{-1}$  for all compositions showed a decrease in intensity with the increase in the dose, indicating fragmentation of sulfone group and aryl ether group.

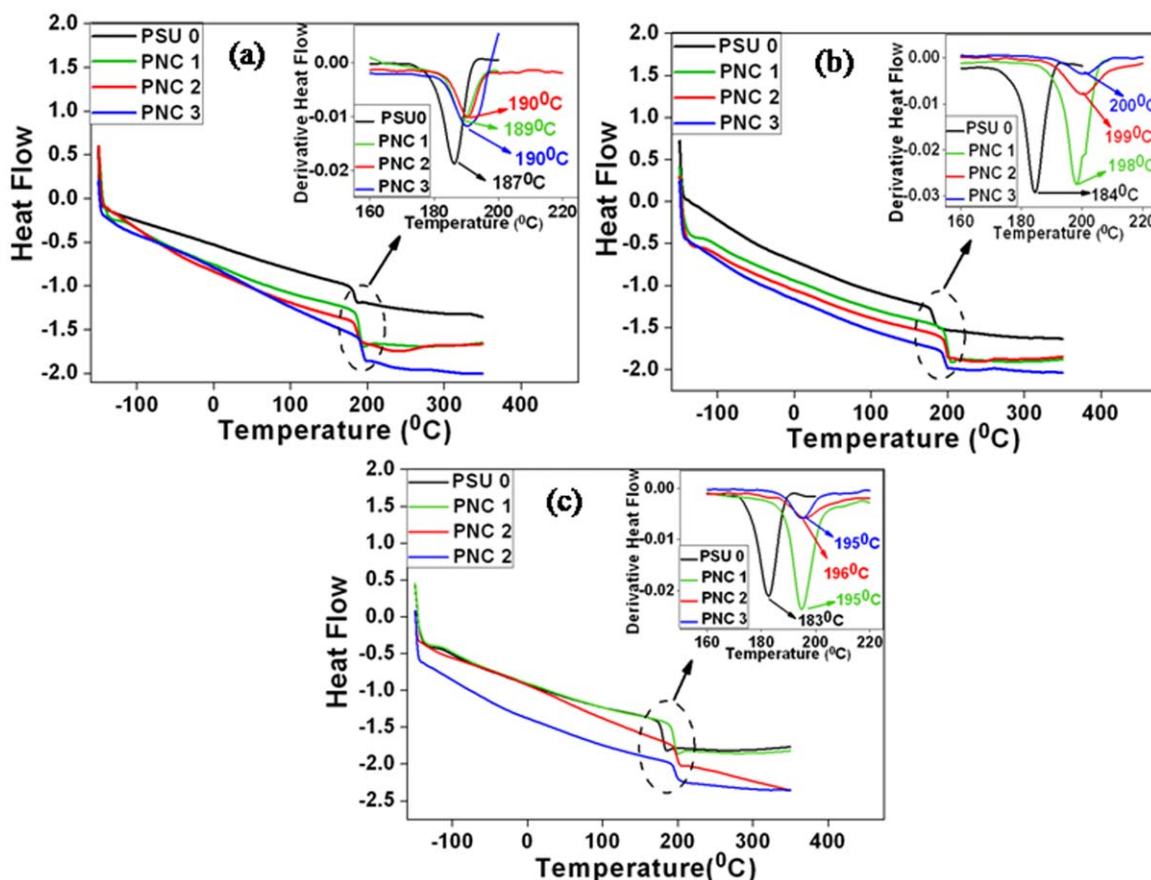
### DSC Studies

Figure 3 shows the DSC thermograms of neat PSU as well as PSU/MWCNT nanocomposites at different weight percent of MWCNT unexposed to  $\gamma$  radiation. Pristine PSU has a glass transition temperature ( $T_g$ ) of  $187^\circ\text{C}$ , but addition of MWCNT increases the  $T_g$  to  $190^\circ\text{C}$ .

Glass transition temperature of polymer or polymer composite depends on the free volume. The incorporation of fillers in the polymer matrix can either increase or decrease the free volume leading to changes in the  $T_g$ .

If a polymer has a higher affinity to filler, it will demonstrate reduced mobility and reduced free volume and a higher  $T_g$ .<sup>31</sup> Momeni and Pakizeh<sup>32</sup> have shown that increase in MgO nanoparticles loading in PSU matrix increased the  $T_g$  of PSU.

In another work by Pham *et al.*,<sup>33</sup> for Polystyrene/SWCNT-based nanocomposites, the  $T_g$  was found to increase by  $\sim 3^\circ\text{C}$



**Figure 3.** DSC thermograms of PSU and PSU/MWCNT nanocomposites at (a): 0 MGy, (b): 1 MGy and (c): 2 MGy. [Color figure can be viewed in the online issue, which is available at [wileyonlinelibrary.com](http://wileyonlinelibrary.com).]

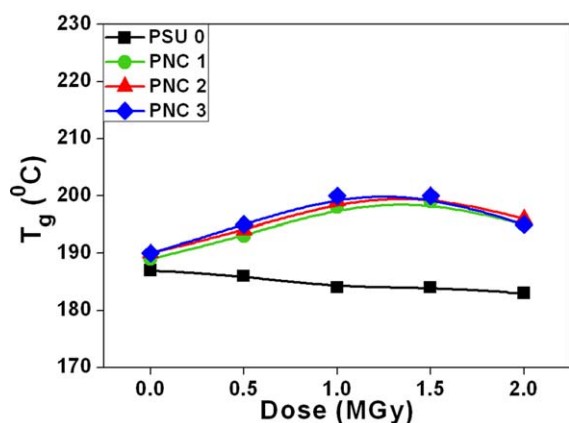


**Figure 4.** The effect of radiation dose on glass transition temperature of PSU and PSU/MWCNT nanocomposites. [Color figure can be viewed in the online issue, which is available at [wileyonlinelibrary.com](http://wileyonlinelibrary.com).]

with increase in SWCNT content for the bulk of the nanocomposites, while films thinner than 45 nm, the  $T_g$  decreased with the decrease in the film thickness. Similar observations have been reported by Guerin and Prud'homme.<sup>34</sup> Particular fillers can interact differently with different polymers and can show

different behavior of  $T_g$ .<sup>35</sup> These differences were attributed to surface wetting.

The decrease in  $T_g$  can be due to various reasons. Incorporation of nanoparticles can increase the free volume and hence a decrease in  $T_g$ .<sup>36</sup> Nanoparticle size can play an important role in the reduction of  $T_g$ . Ash *et al.*<sup>37</sup> found that addition of alumina nanoparticles to poly(methyl methacrylate) decreased the  $T_g$  by almost 25°C. Further, 17nm particles at a lower wt % were more effective in reducing the  $T_g$  than the 38 nm particles. This was found to depend on the interfacial area between the particles and the polymer.

In this case, the marginal increase in  $T_g$  with the increase in wt % of MWCNT is possibly due to interaction between the polymer and the MWCNT. Similar trend is shown for the PSU nanocomposites exposed to 1 MGy as well as 2 MGy of dose. The insets in the Figure 3(a–c) show the derivative thermograms. The behavior of derivative heat flow of PNC1 exposed to 1 MGy and 2 MGy of gamma radiation [insets in the Figure 3(b,c)] differs when compared with other samples (PNC 2 and PNC 3). It is likely that initial interaction between PSU and MWCNT is less. On exposure to  $\gamma$ -radiation, the entanglements formed between the free radicals of PSU and MWCNT is weak. During heating process, a large

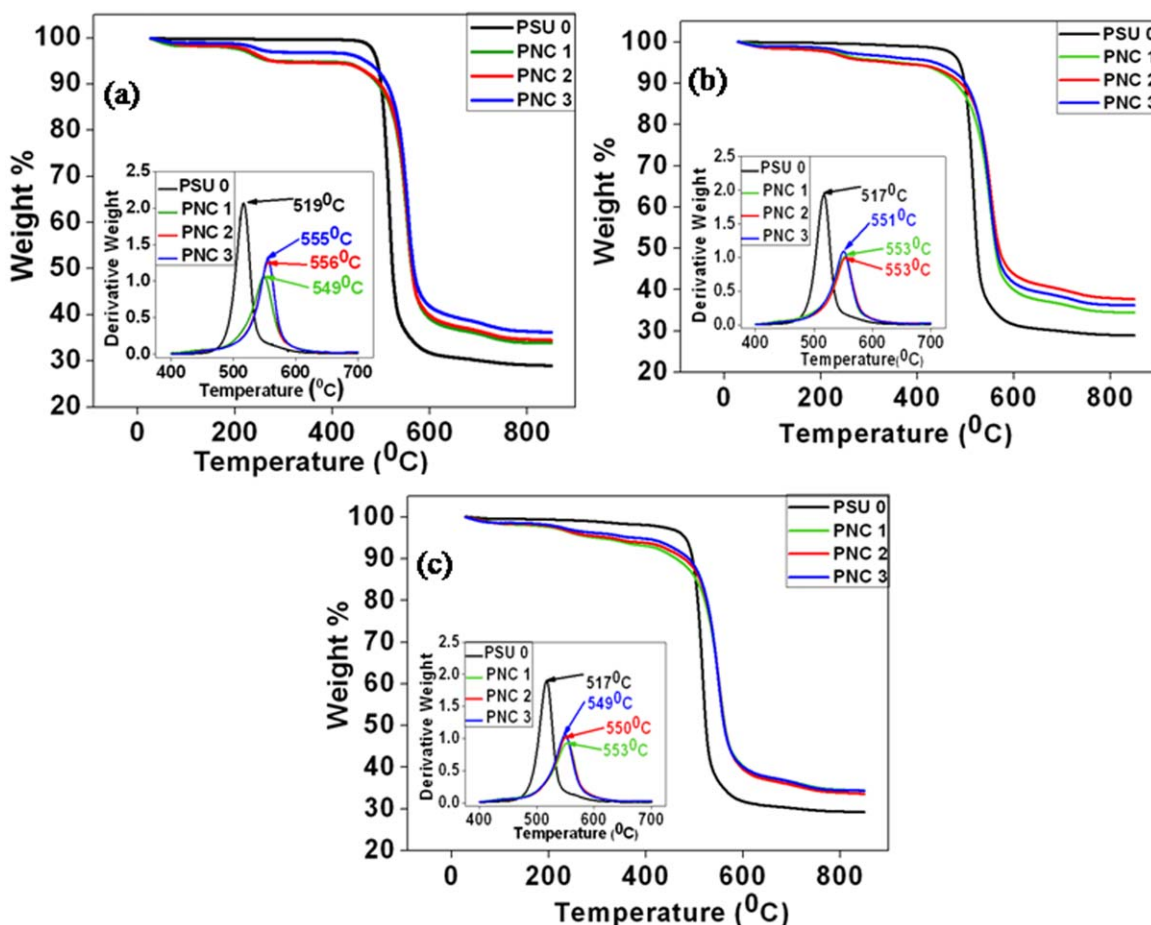


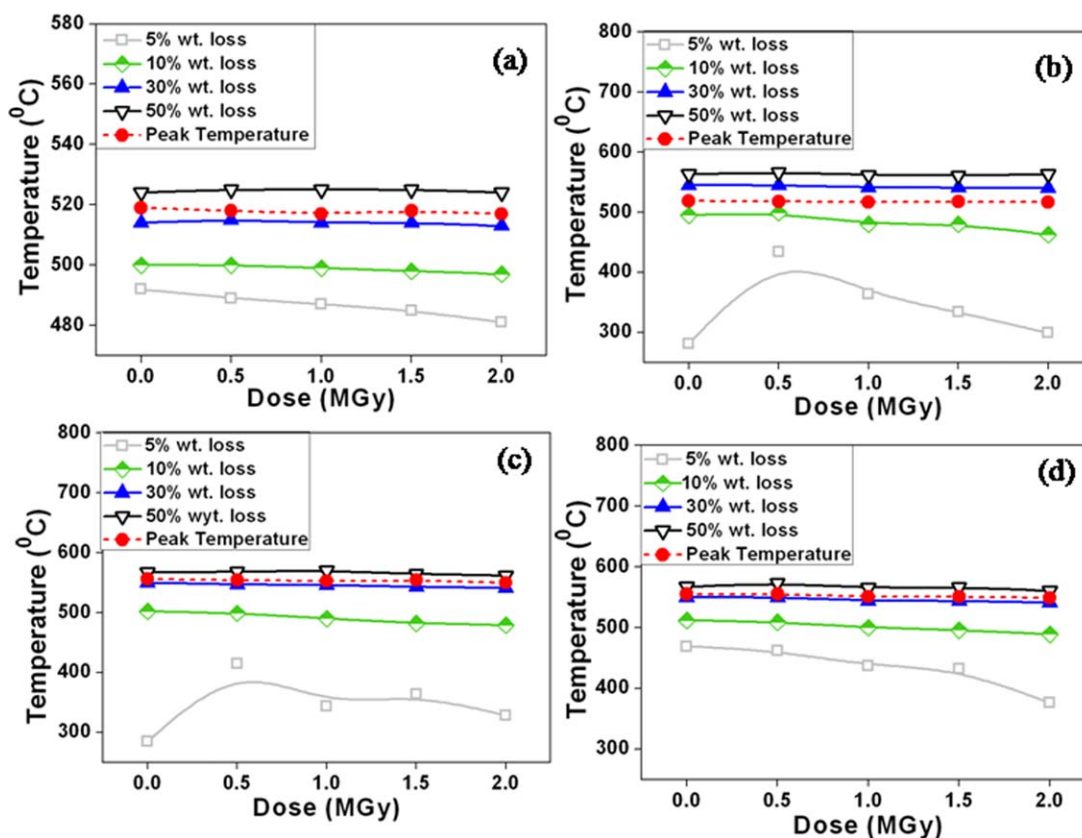
**Figure 5.** TGA and DTG thermograms of PSU and PSU/ MWCNT nanocomposites at (a): 0 MGy, (b): 1 MGy and (c): 2 MGy. [Color figure can be viewed in the online issue, which is available at [wileyonlinelibrary.com](http://wileyonlinelibrary.com).]

**Table III.** (a) Thermal Data from TGA for Exposure at 0 MGy; (b) THERMAL Data from TGA for Exposure at 1 MGy; (c) Thermal Data from TGA for Exposure at 2 MGy.

Material	$T_5$ (°C)	$T_{10}$ (°C)	$T_{20}$ (°C)	$T_{30}$ (°C)	$T_{40}$ (°C)	$T_{50}$ (°C)	$T_{peak}$ (°C)
(a)							
PSU 0	492	500	508	514	519	524	519
PNC 1	281	495	532	545	554	563	549
PNC 2	278	498	534	547	556	564	556
PNC 3	469	512	539	550	558	567	555
(b)							
PSU 0	487	499	508	514	519	525	517
PNC 1	364	480	524	541	552	562	553
PNC 2	344	490	531	546	556	570	553
PNC 3	437	500	531	544	554	565	551
(c)							
PSU 0	481	497	507	513	519	524	517
PNC 1	299	463	521	540	552	563	553
PNC 2	328	479	525	541	551	562	550
PNC 3	376	489	526	541	551	561	549

amount of heat is absorbed to strengthen the interaction between the free radicals of PSU and MWCNT, which explains the difference in the observed derivative heat flow of PNC 1 compared with PNC 2 and PNC 3.

Figure 4 shows the changes in glass transition temperature of pristine PSU as well as PSU/MWCNT nanocomposites with radiation dose. For pristine PSU, the decrease in  $T_g$  with dose is marginal. This is due generation of low molecular weight

**Figure 6.** Temperature changes at different weight loss percent (from TGA thermograms) with dose of (a): PSU 0, (b): PNC 1, (c): PNC 2, and (d): PNC 3. [Color figure can be viewed in the online issue, which is available at wileyonlinelibrary.com.]

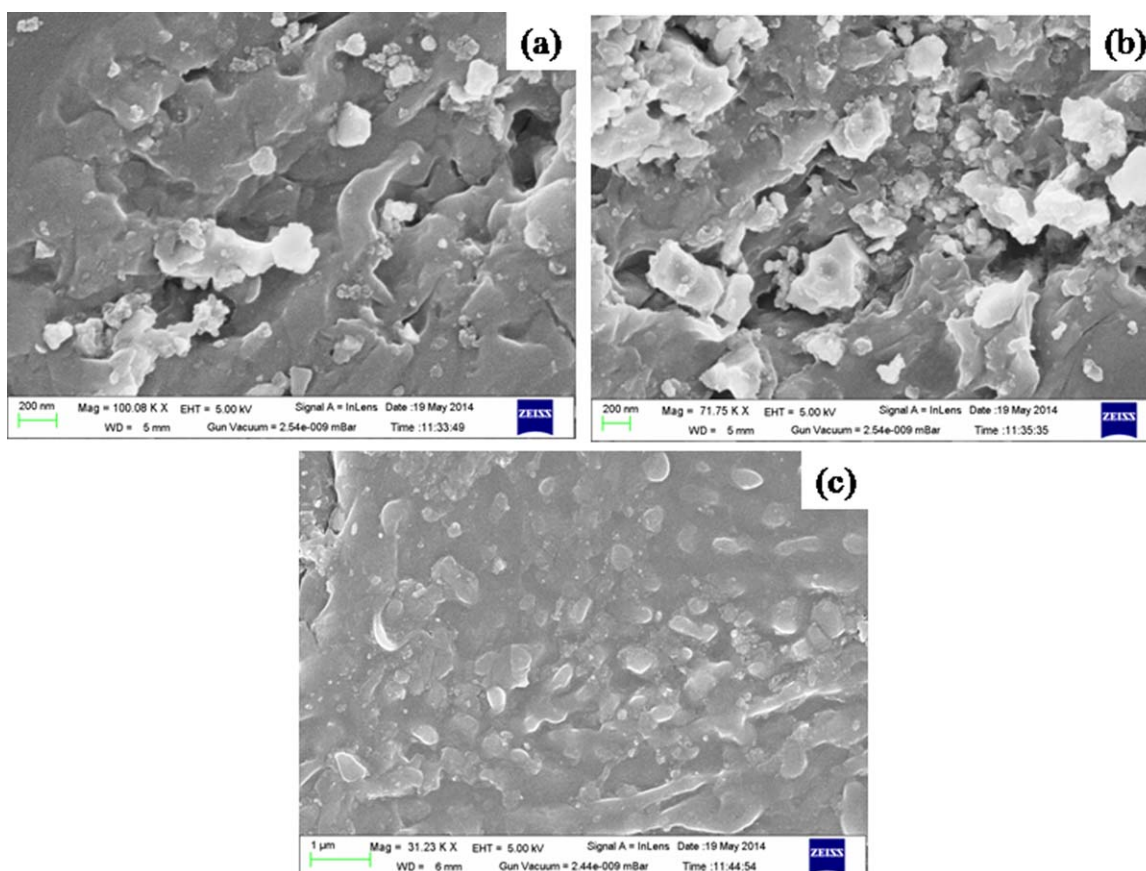


**Figure 7.** Cryo-fractured FESEM image of a: PNC 1, b: PNC 2 and c: PNC 3. [Color figure can be viewed in the online issue, which is available at [wileyonlinelibrary.com](http://wileyonlinelibrary.com).]

fragments (as seen from the GPC trace analysis) due to degradation of PSU.<sup>22,24</sup> For a given composition of PSU/MWCNT nanocomposite, the  $T_g$  increases up to 1.5 MGy and then decreases. During the irradiation process, free radicals are generated [23]. As mentioned earlier, MWCNT act as free radical scavenger.<sup>28–30</sup> The free radicals generated would interact with MWCNT and form entanglements. This would reduce the mobility of the polymer chains as well as the free volume and increase the  $T_g$ .

#### TGA Studies

Figure 5(a–c) shows the TGA as well as the derivative thermogram plots while Table III gives the TGA data from thermograms.

In case of unirradiated PSU, the onset of degradation (corresponding to 5% weight loss:  $T_5$ ) is 492°C. With increase in the MWCNT content (up to 1 wt %), the onset temperature decreases and again increases for 2 wt % of MWCNT, but is less than that of pristine PSU (Table III). A similar trend is also observed at 10% weight loss. This decrease is likely due to weak van der Waals forces of attraction between the MWCNT's and the trapped solvent vapours in the bulk of the material<sup>38</sup>. Subsequently, on application of heat, these solvent vapours tend to diffuse through the bulk of the material and show up as onset of degradation at lower temperatures. Once the entrapped sol-

vent leaves the bulk of the material, the CNTs tend to hinder the segmental motion of the polymer chain, possibly due to  $\pi$ - $\pi$  interactions between the CNT and PSU.<sup>25</sup> This leads to steady increase in the weight loss temperature with the increase in the MWCNT content. The presence of MWCNT's could also introduce new means of energy dissipation such as disruption of secondary interactions with polymers which would alternatively contribute to an increased degradation temperature. The temperature corresponding to 20, 30, 40, and 50% weight loss from the TGA scans shows a similar trend. Further, with the increase in MWCNT content, the peak temperature (temperature at maximum degradation rate) shifts towards the higher temperature. This trend can be observed from Figure 6(b,c) as well Table III for PSU/ MWCNT nanocomposites exposed to 1 MGy as well as 2 MGy dose.

Figure 6 shows the temperature corresponding to weight loss at 5, 10, 30, and 50% as well as peak temperature for pristine PSU as well as PSU nanocomposites with change in dose, obtained from the TGA thermo-grams.

The temperatures corresponding to 5 and 10% weight loss for PSU marginally decreased and remained constant at higher weight loss with an increase in dose [Figure 6(a)]. This is attributed to degradation of PSU.<sup>23</sup> For the nanocomposites corresponding to 0.5 and 1 wt % of MWCNT, temperatures

**Table IV.** Mechanical Properties of PSU and Its Nanocomposites at Different Dose

Composition	Dose (MGy)	Tensile strength at peak load (MPa)	Elongation at break (%)
PSU 0	0	71	25
	0.5	68	19
	1.0	67	12
	1.5	65	8
PNC 1	0	74	15
	0.5	72	11
	1.0	60	8
	1.5	52	7
PNC 2	0	76	13
	0.5	71	10
	1.0	66	7
	1.5	58	5
PNC 3	0	78	10
	0.5	73	8
	1.0	69	6
	1.5	63	4

corresponding to 5% weight loss showed an increase with dose up to 0.5 MGy and thereafter decreased [Figure 6(b,c)]. This is possibly due to the  $\pi$ - $\pi$  interactions between the CNT and PSU<sup>25</sup> after the diffusion of the entrapped solvent. A subsequent increase in dose weakens this interaction and also degrades the PSU matrix, and hence a decrease in the temperature. For temperatures corresponding to weight loss at other percentage, a marginal decrease is observed with increase in dose, which is due to degradation of PSU. For 2 wt % MWCNT [Figure 6(d)], with increase in dose, the temperature corresponding to 5, 10, 30, and 50% weight loss decreased which is due to degradation.

#### FESEM

To understand the morphology and the distribution of the MWCNT in PSU as well as have idea about the existence of any physical interaction between, FESEM was used. Figure 7 shows the cryo-fractured surface micrographs of PSU/MWCNT nanocomposites. From these micrographs, it is clearly seen that most of MWCNTs are dispersed individually in PSU matrix. Further, the existence of PSU matrix on the surface of MWCNT suggests a good interfacial attraction between MWCNT and PSU matrix, though few isolated MWCNT are observed.

#### Mechanical Properties

The mechanical properties of PSU and its nanocomposites are given in Table IV. MWCNT concentration as well as radiation dose have notable impacts on mechanical properties. On increasing the MWCNT wt %, the tensile strength (at peak load) is observed to increase from 71 MPa to 78 MPa, indicating an improvement of 10% in strength. The increase can be attributed to two things: good dispersion of MWCNT in the PSU matrix and interfacial adhesion between the PSU matrix and the CNTs, which helps in transfer of load from the polymer to the CNTs.

With increased dose, a decrease in tensile strength was observed for the neat PSU as well as PSU nanocomposites. For neat PSU, the tensile strength decreased from 71 MPa to 65 MPa (7% decrease). This is mainly due to the degradation of the polymer. For 0.5 wt % of MWCNT, the tensile strength decreased from 74 MPa to 52 MPa (29% decrease), for 1 wt % of MWCNT, the tensile strength decreased from 76 MPa to 58 MPa (24% decrease) and for 2 wt % of MWCNT, the tensile strength decreased from 78 MPa to 63 MPa (19% decrease). This is attributed to degradation of the PSU matrix, which possibly weakens the interfacial adhesion of the PSU matrix with the CNTs and act as points of stress concentration.

Elongation at break decreases with MWCNT content. It is likely that agglomerates of MWCNT present at higher wt % acts as defects and weakens the interfacial adhesion between PSU and MWCNT. With increase in dosage, the decrease is due to degradation of PSU which further adds to weakening of adhesion. It was not possible to make the measurements beyond 1.5 MGy, particularly for the PSU/MWCNT nanocomposites, as brittle fracture of specimens occurred during setting and testing of specimens.

#### SUMMARY AND CONCLUSIONS

PSU/MWCNT nanocomposite films were prepared by a solution casting process. Morphological studies using FESEM indicates good dispersion of MWCNTs in the PSU matrix. The prepared films were subjected to  $\gamma$ -radiation in an argon environment in order to avoid the effect of air/oxygen on PSU/MWCNT nanocomposites during the irradiation process. The irradiated films were characterized for various properties. GPC analysis shows decrease in molecular weight on exposure to radiation. This is due to degradation of PSU due to chain scission. IR spectroscopy shows an overall increase in intensity in the entire spectral range for neat PSU. This is due to degradation of PSU which is further confirmed by the decrease in intensity of bands at 3100, 2950, 1325, 1290, and 1230  $\text{cm}^{-1}$ , respectively. A new band due to  $>\text{C}=\text{O}$  group appears at  $\sim 1730 \text{ cm}^{-1}$ . In case of PSU/MWCNT nanocomposites, no degradation was observed for the aromatic rings. The band at 1730  $\text{cm}^{-1}$  showed a shift towards 1680  $\text{cm}^{-1}$  due to possible interaction of  $>\text{C}=\text{O}$  group with MWCNT. The bands at 1450, 1325, 1290, and 1145  $\text{cm}^{-1}$  showed a decrease in intensity with increase in dose due to fragmentation of methylene, sulfone, and aryl ether groups. DSC thermograms revealed dose-related changes. For neat PSU a decrease in  $T_g$  was observed with increase in dosage, which is attributed to its degradation and also confirmed by GPC trace analysis. For PSU/MWCNT nanocomposites, the increase in MWCNT content and dose up to 1.5 MGy increased the  $T_g$ . The increase in  $T_g$  with MWCNT content is due to  $\pi$ - $\pi$  interaction between the aromatic rings of PSU and MWCNT. The increase in  $T_g$  with dosage is possibly due to free radical scavenging effect of MWCNT. TGA thermograms showed a marginal increase in thermal stability with MWCNT wt % but a decrease was observed for neat PSU as well as PSU/MWCNT nanocomposites with dosage. Tensile strength increased with MWCNT content but decreased with dosage. Elongation at break showed a decrease with MWCNT content as well as radiation dose.



## REFERENCES

1. Ajayan, P. M.; Banhart, F. *Nat. Mater.* **2004**, *3*, 135.
2. Filleter, T.; Bernal, R.; Li, S.; Espinosa, H. D. *Adv. Mater.* **2011**, *23*, 2855.
3. Filleter, T.; Espinosa, H. D. *Carbon* **2013**, *56*, 1.
4. Peng, B.; Locascio, M.; Zapol, P.; Li, S.; Mielke, S. L.; Schatz, G. C.; Espinosa, H. D. *Nat. Nanotechnol.* **2008**, *3*, 626.
5. Miao, M. H.; Hawkins, S. C.; Cai, J. Y.; Gengenbach, T. R.; Knott, R.; Huynh, C. P. *Carbon* **2011**, *49*, 4940.
6. Miko, C.; Milas, M.; Seo, J. W.; Gaal, R.; Kulik, A.; Forro, L. *Appl. Phys. Lett.* **2006**, *88*, 151905.
7. Qin, S. H.; Qin, D. Q.; Ford, W. T.; Zhang, Y. J.; Kotov, N. A. *Chem. Mater.* **2005**, *17*, 2131.
8. Wang, C. Y.; Chen, T. G.; Chang, S. C.; Cheng, S. Y.; Chin, T. S. *Adv. Funct. Mater.* **2007**, *17*, 1979.
9. Xu, Z.; Chen, L.; Liu, L.; Wu, X.; Chen, L. *Carbon* **2011**, *49*, 350.
10. Xu, Z.; Min, C.; Chen, L.; Liu, L.; Chen, G.; Wu, N. *J. Appl. Phys.* **2011**, *109*, 054303.
11. Kleut, D.; Jovanović, S.; Marković, Z.; Kepić, D.; Tošić, D.; Romčević, N.; Marinović-Cincović, M.; Dramićanin, M.; Holclajtner-Antunović, I.; Pavlović, V.; Dražić, G.; Milosavljević, M.; Todorović Marković, B. *Mater. Character.* **2012**, *72*, 37.
12. Wu, W. T.; Lei, S.; Wang, Y.; Pang, W.; Zhu, Q. *Nanotechnology* **2008**, *19*, 125607.
13. Xu, H. X.; Wang, X. B.; Zhang, Y. F.; Liu, S. Y. *Chem. Mater.* **2006**, *18*, 2929.
14. Martínez-Morlanes, M. J.; Castell, P.; Martínez-Nogués, V.; Martínez, M. T.; Alonso, P. J.; Puértolas, J. A. *Compos. Sci. Technol.* **2011**, *71*, 282.
15. Hossam, M. S. *J. Radiat. Res. Appl. Sci.* **2013**, *6*, 11.
16. Clayton, L.; Gerasimov, T.; Harmon, J. P. *Polym. Bull.* **2004**, *52*, 259.
17. Tatro, S. R.; Clayton, L.; O'Rourke Muisener, P. A.; Rao, A. M.; Harmon, J. P. *Polymer* **2004**, *45*, 1971.
18. O'Rourke Muisener, P. A.; Clayton, L.; D'Angelo, J.; Harmon, J. P.; Sikder, A. K.; Kumar, A.; Cassell, A. M.; Meyyappan, M. *J. Mater. Res.* **2002**, *17*, 2507.
19. Stevens, M. P. In *Polymer Chemistry: An Introduction*, 3rd ed.; Oxford University Press: Oxford, **1999**, p. 311.
20. Kim, S.; Chen, L.; Johnson, J. K.; Marand, E. *J. Membr. Sci.* **2007**, *294*, 147.
21. Nayak, L.; Rahaman, M.; Khastgir, D.; Chaki, T. K. *Polym. Bull.* **2011**, *67*, 1029.
22. Brown, J. R.; O'Donnell, J. H. *J. Appl. Polym. Sci.* **1979**, *23*, 2763.
23. Steckenreiter, T.; Balanzat, E.; Fuess, H.; Trautmann, C. *J. Polym. Sci. Part A: Polym. Chem.* **1999**, *37*, 4318.
24. Brown, J. R.; O'Donnell, J. H. *J. Appl. Polym. Sci.* **1975**, *19*, 405.
25. Li, H. M.; Fouracre, R. A.; Given, M. J.; Banford, H. M.; Wysocki, S.; Karolczak, S. *IEEE Trans. Dielectrics Electrical Insulation* **1999**, *6*, 295.
26. Reid, B. D.; Ruiz-Trevino, F. A.; Musselman, I. H.; Balkus, K. J., Jr; Ferraris, J. P. *Chem. Mater.* **2001**, *13*, 2366.
27. Brown, J. R.; O'Donnell, J. H. *J. Appl. Polym. Sci.* **1975**, *19*, 405.
28. Huskic, M.; Zigon, M. *Eur. Polym. J.* **2007**, *43*, 4891.
29. Martínez-Morlanes, M. J.; Medel, F. J.; Mariscal, M. D.; Puértolas, J. A. *Polym. Test* **2010**, *29*, 425.
30. Watts, P. C. P.; Fearon, P. K.; Hsu, W. K.; Billingham, N. C.; Kroto, H. W.; Walton, D. R. M. *J. Mater. Chem.* **2003**, *13*, 491.
31. Kodjie, S. L.; Li, L.; Li, B.; Cai, W.; Li, C. Y.; Keating, M. J. *Macromol. Sci. Part B: Phys.* **2006**, *45*, 231.
32. Momeni, S. M.; Pakizeh, M. *Brazilian J. Chem. Eng.* **2013**, *30*, 589.
33. Pham, J. Q.; Mitchell, C. A.; Bahr, J. L.; Tour, J. M.; Krishnamurthi, R.; Green, P. F. *J. Polym. Sci. Part B: Polym. Phys.* **2003**, *41*, 3339.
34. Guerin, G.; Prud'homme, R. E. *J. Polym. Sci. Part B: Polym. Phys.* **2007**, *45*, 10.
35. Rittigstein, P.; Torkelson, J. M. *J. Polym. Sci. Part B: Polym. Phys.* **2006**, *44*, 2935.
36. Mackay, M. E.; Dao, T. T.; Tuteja, A.; Ho, D. L.; Horn, B. v.; Kim, H. C.; Hawker, C. J. *Nature Mater.* **2003**, *2*, 762.
37. Ash, B. J.; Seigel, R. W.; Schadler, L. S. *J. Polym. Sci. Part B: Polym. Phys.* **2004**, *42*, 4371.
38. Vaudreuil, S.; Labzour, A.; Ray, S. S.; Mabrouk, K. E.; Bousmina, M. *Nanosci. Nanotechnol.* **2007**, *7*, 2349.